Cerebral Biopsies Using a Photogrammetric Probe Simulator

Michel Boulianne
Département des sciences géodésiques et de télédétection, Université Laval, Ste-Foy, Québec G1K 7P4, Canada
Louis Cloutier
Département de génie mécanique, Université Laval, Ste-Foy, Québec G1K 7P4, Canada
Sanjib K. Ghosh
Département des sciences géodésiques et de télédétection, Université Laval, Ste-Foy, Québec G1K 7P4, Canada

ABSTRACT: Functional neurosurgery such as stereotactic biopsies, interstitial irradiation, chronic depth electrodes, neurostimulator, or drug injection requires the implantation of cerebral probes through the labyrinth of arteries and veins. Current methods used to determine the zones free from blood vessels that can be retained as safe passages for the probe to avoid internal cerebral hemorrhages either lack precision or introduce certain limits. This paper presents a newly developed method aimed at facilitating dependable implantation of cerebral probes. It results from an interdisciplinary research and is based on applying stereophotogrammetric techniques in radiography. An apparatus permitting stereoscopic vision of a floating line has been developed. It permits one to simulate probe implantations. A unique three-dimensional coordinate reference system is used for the whole medical procedure. Clinical tests consisting of 43 brain tumor biopsies carried out on 26 human patients have shown a 100 percent success rate.

INTRODUCTION

In functional neurosurgery, whether, for example, a sample of grey matter is cut off through a biopsy or cerebral waves are analyzed using chronic depth electrodes, the neurosurgeon must introduce a rigid rectilinear probe into the brain of his patient. This operation must be done without running against or, even worse, cutting any blood vessel; otherwise, internal cerebral hemorrhages would result. The search for a safe passage of the probe through the labyrinth of arteries and veins is best done with conventional radiographs of blood vessels (angiographs). This arises from the inability of other bio-imaging systems such as Computed Tomography (CT) or Nuclear Magnetic Resonance (NMR) scanners to provide well defined images of the blood vessels. Current practices of implanting a probe are constrained into the direction perpendicular to the radiographs of the skull profile (Talairach, 1974; Bouvier *et al.*, 1976). Because certain regions of the brain are less vascular than others and because certain tumors can not be accessed via the direction perpendicular to the profile, the neurosurgeons have always dreamed of a tool allowing implantations in all possible directions.

This paper presents a rigorous technique to facilitate the safe implantation of probes through the brain. Emphasis is given to a new photogrammetric device and to the metrical aspects of this method. At the end of the paper the performance of the probe simulator will be evaluated and some clinical cases concerning brain tumor biopsies will be presented.

THE PHOTOGRAMMETRIC PROBE SIMULATION METHOD

Several authors have already proven that it is possible, with rigorous mathematical relations, to determine the position of a point when using stereoscopic radiographs (Sherlock and Aitken, 1980; Boulianne, 1983; Marcotte, 1984). Based on these results, a method to localize a straight line in a given space has been developed. It consists essentially of the application of stereophotogrammetric procedures to radiographs. To support the new method, an apparatus called the "Probe Simulator" has been developed, clinically tested, and patented (U.S.A. patent No. 4.614.499, Canada patent No. 1 246 744). It permits one to simulate, anywhere in the stereoscopic model of the brain, the probe to be implanted, allowing the surgeon to find the safest path for the operation.

The following describes in detail the different phases of the surgical process to make the probe implantation less hazardous (Figure 1).

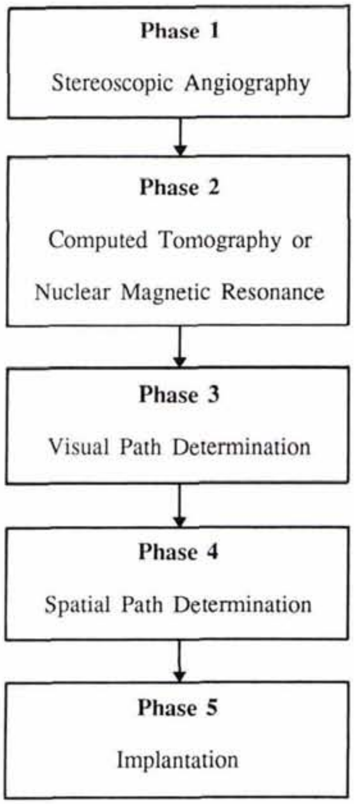

FIG. 1. Phases of the surgical process.

PHOTOGRAMMETRIC ENGINEERING & REMOTE SENSING,
Vol. 57, No. 10, October 1991, pp. 1347–1354.

0099-1112/91/5710–1347$03.00/0

Phase 1: Stereoscopic Angiography

The first phase consists of making stereoscopic radiographs of the cerebral blood vessels, also called angiographs (Figure 2). If the X-ray source and the film holder are held at fixed positions, the radiographic room can be considered as an "X-ray camera" and the usual photogrammetric processing for recovering the spatial information can easily be adapted. In radiography, one basic problem is to establish a three-dimensional (3-D) reference system (Gibaud *et al.*, 1982). For this purpose, a frame maintaining the patient's head fixed during the operation and defining the 3-D coordinate reference system has been designed and built. This frame, called "stereotactic frame", is anchored to the skull with four carbon fiber pins (Figure 3). Two different calibration cubes are successively attached to this frame–one for the angiography (Figure 4) and the other for the computed tomography (Figure 5)–while the frame, being constant, provides the unique system of reference.

Angiographs are produced by injecting a radio-opaque dye, usually iodine, into the blood stream. Because the quantity of dye needed to make all the cerebral blood vessels opaque at the same time would be harmful for the patient, radiologists prefer taking a series of radiographs to collect all the information about the blood vessels. In practice, they inject a small quantity of dye in the arteries and take a series of five to ten radiographs in about 10 seconds. Due to the dye circulation, the first radiographs show the artery network and the last ones present the vein network. In order to produce the stereopairs, the patient's head is tilted about 10 degrees and the process is repeated (Figure 6). Afterwards, the physicians select the best two pairs showing the arteries and the veins, respectively. Then these two stereoscopic pairs are placed in such a way on the probe simulator transparent table that a simple translation of the mirror stereoscope allows the 3-D vision of the blood vessel networks (Figure 7).

To define the reference system during the angiographic phase, a few control points are set in strategic places on the calibration frame (Figure 4). One must pay special attention concerning the location of these points; otherwise, the patient's skull or a blood vessel could hide the control. Small lead balls are suitable for these points (0.5 mm in diameter). The 3-D coordinate system is used throughout the complete surgical process. Also, to provide a radiographic coordinate reference system, four lead balls are placed on the film case and used as fiducial marks.

Phase 2: Computed Tomography

In the next phase the patient is moved to the Computed Tomography (CT) room (Figure 8). This system produces images of thin slices of the brain (usually in the neighborhood of 3 mm thick). As previously mentioned, the blood vessels are not visible on the CT images but, in contrast to conventional radiographs, the tumors can be seen (Figure 9). Both systems can provide very valuable information to the surgeon and therefore are perfectly complementary. The CT scanner shows the tumor to be investigated but, in order to be useful, the spatial position of the tumor has to be related to the same reference system as defined in the first phase for the angiography. A special non-metallic frame is attached to the main frame to establish the reference system on each slice (Figure 5). The calibration cube used for the angiography with the lead balls is not suited for the CT scanner because any metallic objects produce artefacts in the image. The design of the CT calibration cube is such that the height of each slice is easily computed. Three diagonal rods made of carbon fibers give the spatial position of three points defining the plane corresponding to a given slice.

Once the series of slices have been produced, the surgeon selects the image corresponding to the middle part of the tumor and points at its center on the CT scanner screen with the help of a pointing device such as a rolling ball or a mouse available on every type of medical scanner. By way of measuring the planimetric position of the target and by knowing the equation defining the particular slice, the third coordinate is computed.

Because the tumor cannot be seen on the radiographs showing the blood vessels, the center of the tumor (now precisely located with the CT scanner) is transferred to each stereoradiograph by using the collinearity condition in which all the parameters are estimated in a preliminary X-ray system self-calibration (see phase 4).

It is worth noting that other types of medical scanners, such as Nuclear Magnetic Resonance (NMR) systems, would provide the same information. The physician can also decide to investigate a particular zone of the brain where the blood vessels show an

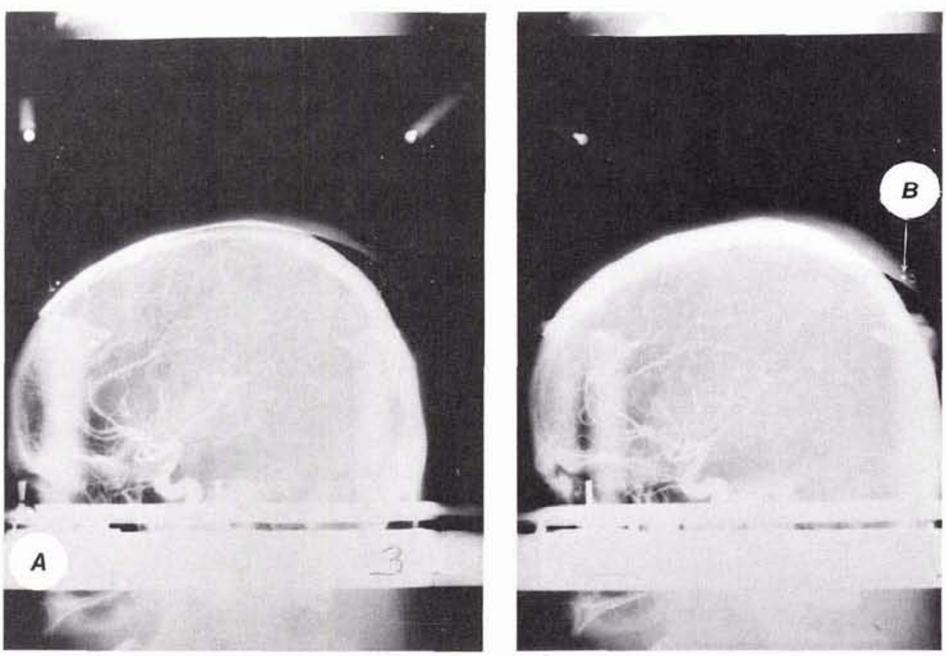

Fig. 2. Arteries stereo-angiograph. (A) Stereotactic frame. (B) Control point. (Courtesy of MEC-INOV Inc. and Enfante-Jésus Hospital)

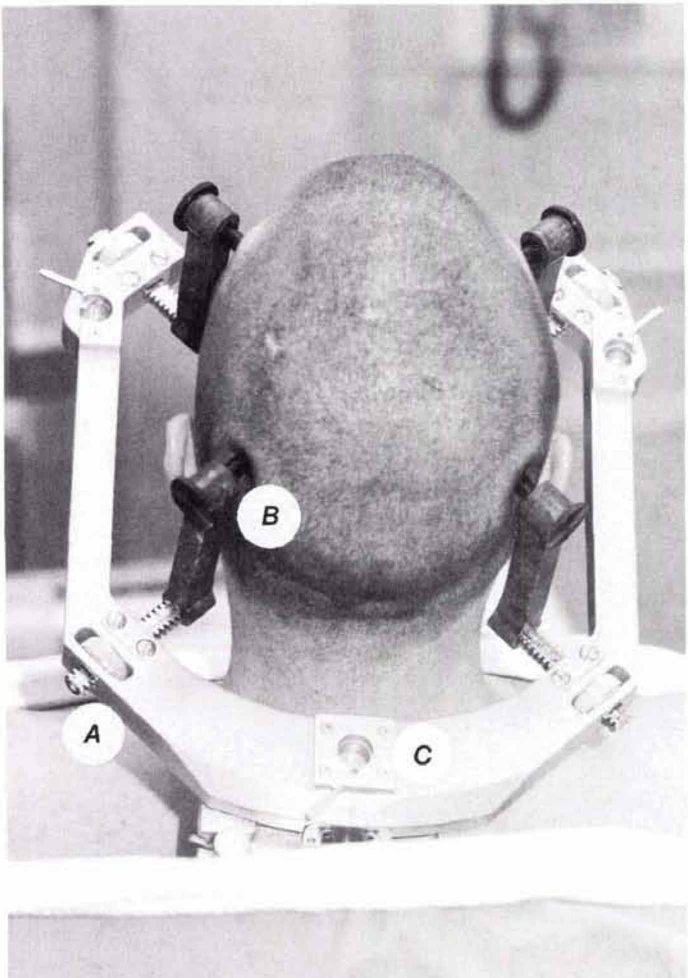

FIG. 3. Stereotactic Frame. (A) Micrometers. (B) Anchor pins. (C) Positioning holes. (Courtesy of MEC-INOV Inc. and Enfant-Jésus Hospital)

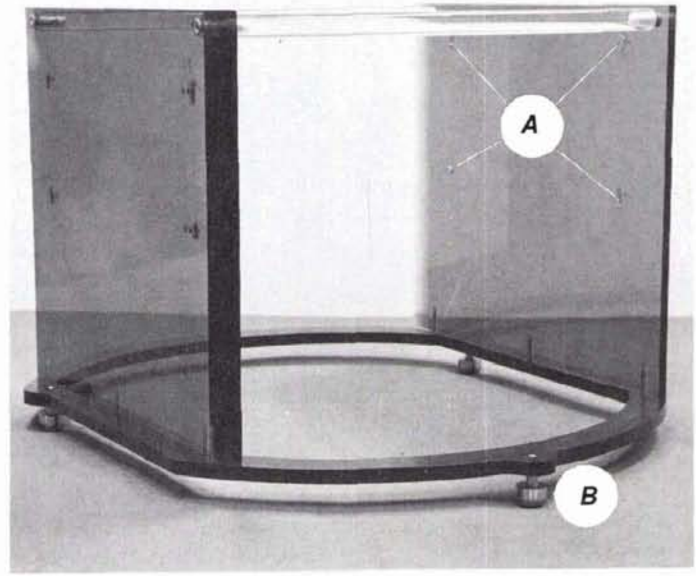

FIG. 4. X-Ray Calibration cube. (A) Lead balls used as control points. (B) Positioning pins. (Courtesy of MEC-INOV Inc. and Enfant-Jésus Hospital)

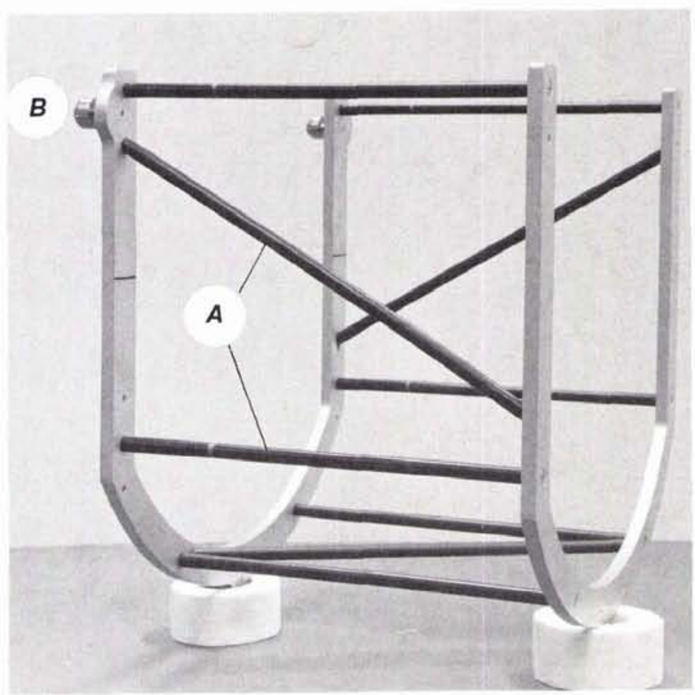

FIG. 5. Computed tomography calibration cube. (A) Carbon fibre rods. (B) Positioning pins. (Courtesy of MEC-INOV Inc. and Enfant-Jésus Hospital)

abnormality without using the scanners. Indeed, the probe simulator described later can be operated freely without prior knowledge of the exact target coordinates.

PHASE 3: VISUAL PATH DETERMINATION

In order to facilitate the determination of safe passage for the implantation of probes through the cerebral blood vessels, a new apparatus named a "Probe Simulator" has been developed (Figure 7).

This device performs three main functions:

- Allow the stereoscopic viewing of the blood vessel networks (arteries and veins).
- Permit the placement at will, in a stereoscopic model of the blood vessels, the image of a line representing the actual probe.
- Record the coordinates (x,y) of the image points on the radiographs.

The "floating line" representing the surgical tool to be implanted is created by superimposing, on each radiograph forming the stereopair, a transparent disc on which a radial line has been engraved. Figure 10 shows the simple, yet efficient, mechanism of the floating line.

To facilitate the positioning of the radiographs on the light table of the simulator, the stereopairs have to be produced in a particular manner. More specifically, the epipolar line has to be parallel to the line defined by the two fiducial marks at the bottom of each radiograph. This way a simple alignment of the four bottom fiducials suffice to recover the stereoscopic vision (Figure 11). This important step reduces significantly the physician's effort, and compensates largely for the mechanical constraint related to the rotation of the patient's head. Also, the vein and artery models being geometrically identical (the only difference is the time of the exposure), it is possible to place the second model at a known distance from the first one

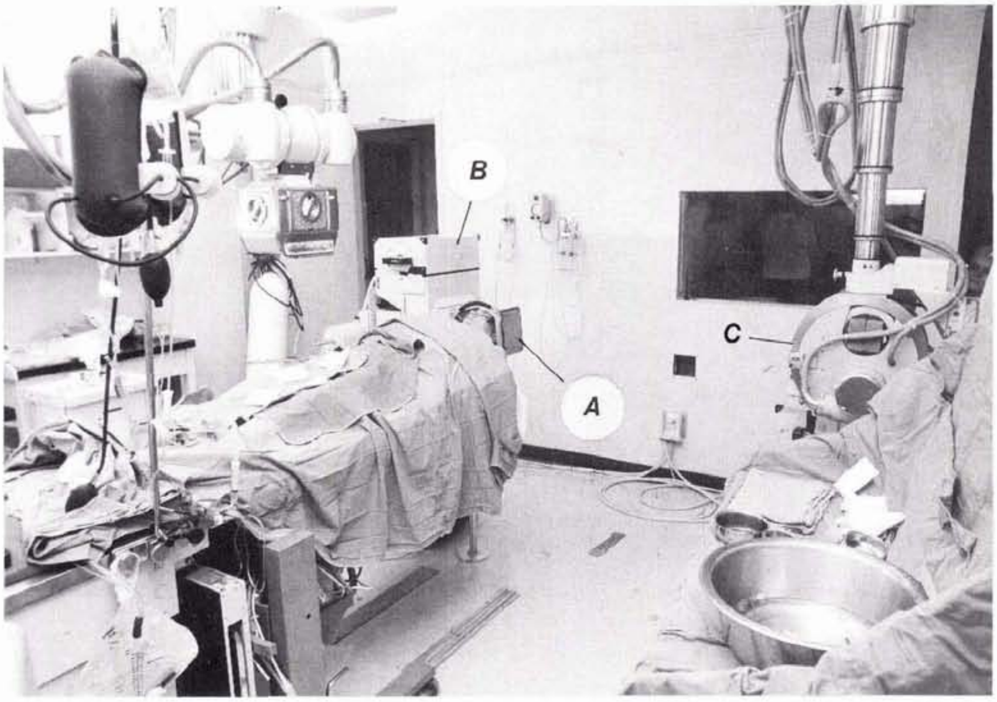

FIG. 6. X-Ray room. (A) X-Ray calibration cube. (B) X-Ray film case. (C) X-Ray source. (Courtesy of MEC-INOV Inc. and Enfant-Jésus Hospital)

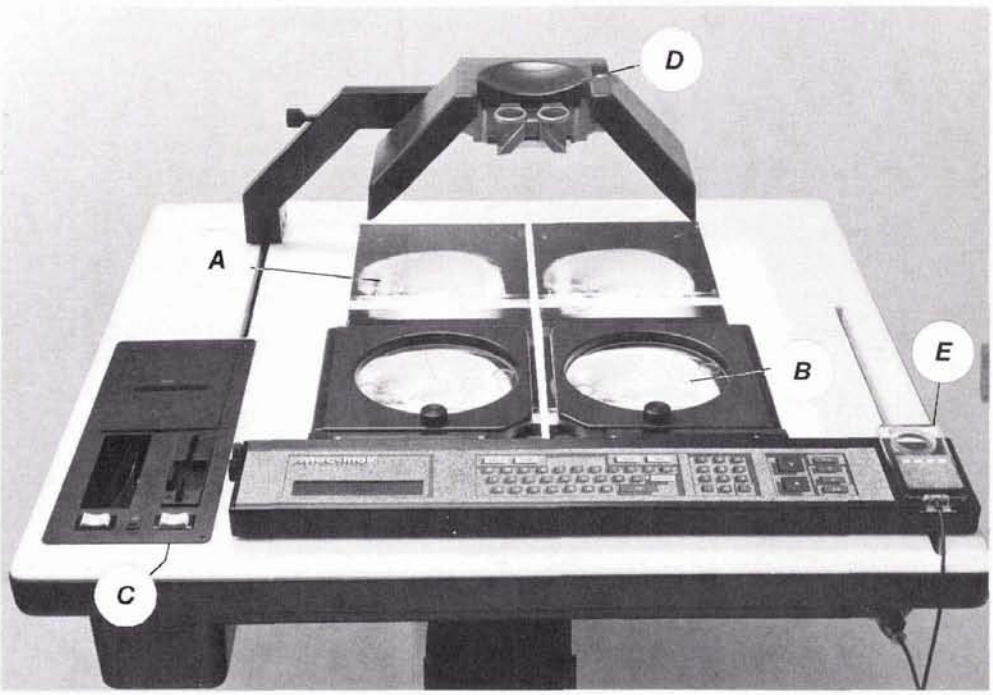

FIG. 7. Probe simulator. (A) Veins angiograph. (B) Arteries angiograph. (C) Micro-computer. (D) Stereoscope. (E) Pointing device. (Courtesy of MEC-INOV Inc. and Enfant-Jésus Hospital)

and view a particular path in both models by an automatic translation of the stereoscope and the floating line mechanism.

With the help of the simulator, the physician can visualize the position of a probe in the cerebral space before its implantation. If there exists a risk of hurting a blood vessel, the operator has only to perform a few simple manipulations (translations and/or rotations) of the two acrylic discs on which appear the images of the pseudo-probe, and the situation is corrected. Because two stereomodels are involved, the surgeon has to look first for a potential path in the artery model and then, with an automatic displacement of the floating line mechanism, he has to verify if the selected passage is also safe for the veins. If a current path selected may be hazardous for a vein, a slight correction is made and the new position is verified for the artery model. This procedure is repeated until the path for the probe is safe for both models. Because the vein network is less dense and less subject to hemorrhages, a few minutes are sufficient to arrive at a visual path determination.

In the process, no constraints are necessary regarding the point of penetration of the probe and its final direction, with the consideration of non-interception of blood vessels.

If the exact image position of the center of the tumor on each

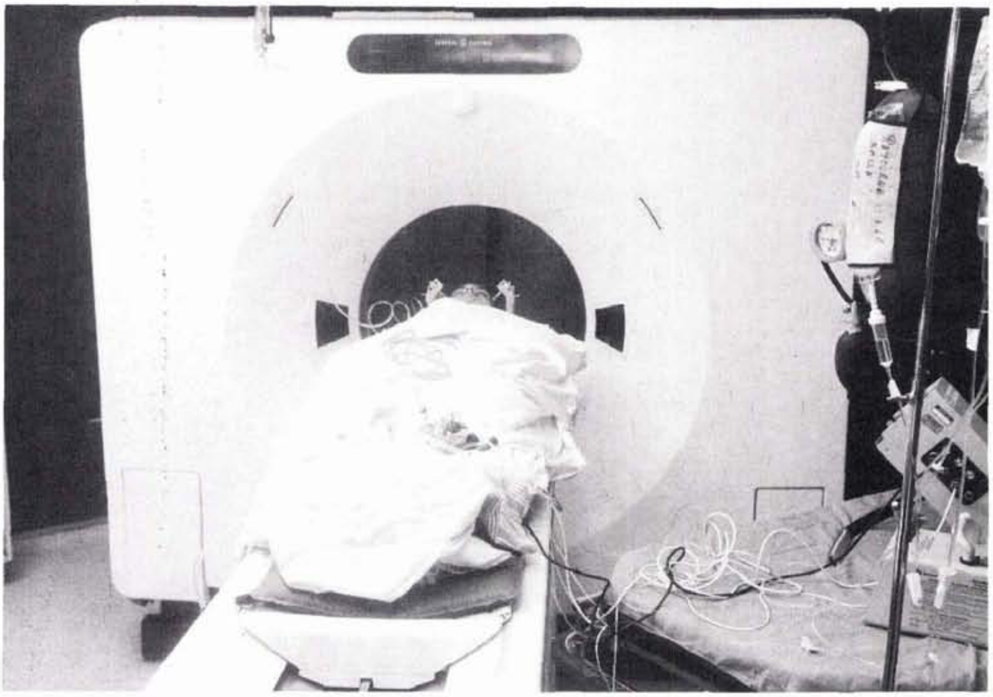

FIG. 8. Computed tomography room. (Courtesy of MEC-INOV Inc. and Enfant-Jésus Hospital)

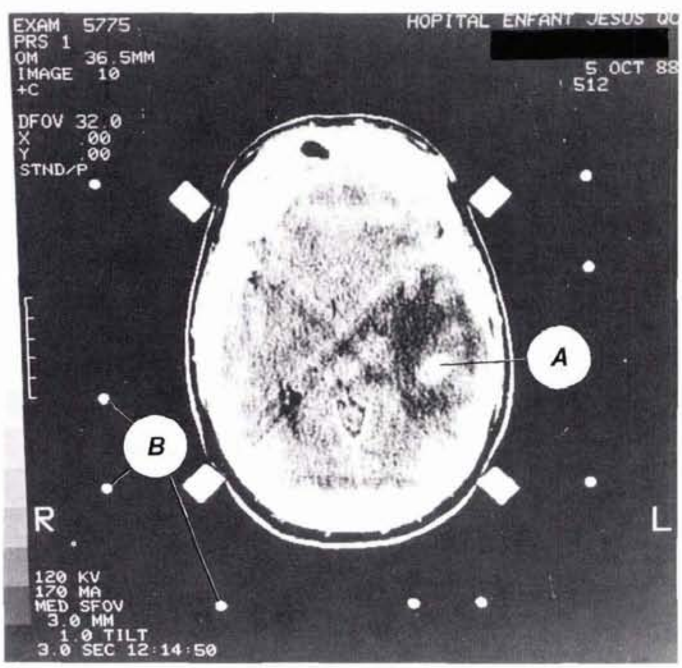

FIG. 9. Brain tomograph. (A) Tumor. (B) Carbon fiber rod. (Courtesy of MEC-INOV Inc. and Enfant-Jésus Hospital)

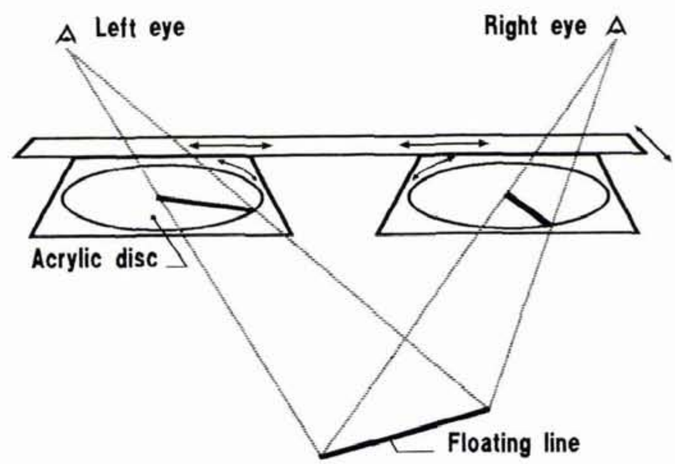

FIG. 10. Floating line concept.

image has been computed from the CT images, the simulator automatically positions the centers of the discs, representing the extremity of the probe, on this exact location. The only duty left to the physician is to locate a safe path to reach the tumor. This is done by rotating the discs about that point until he is convinced that the probe will not hurt any blood vessel.

Once the safe passage has been localized, the coordinates of two points of the floating line are automatically recorded by the precision coordinate digitizer. The digitizer also permits measuring the coordinates of the fiducial marks and calibration points.

It is interesting to note that no special training is necessary to operate the probe simulator; normal stereoscopic vision would suffice.

PHASE 4: SPATIAL PATH DETERMINATION

The fourth phase of the process aims at precise localization of the probe trajectory. This is accomplished by using the self-calibration technique (Brown *et al.*, 1964; Kenefick *et al.*, 1972). According to the philosophy of this method, the inner and outer orientation parameters of the camera are simultaneously estimated with the evaluation of the unknown object coordinates. This approach tends to provide higher precision in the results. The mathematical model of the self-calibration technique is the well-known collinearity equation (Slama, 1980). The preliminary self-calibration carried out in the course of the second phase aimed at the estimation of the parameters needed for the localization of the tumor on the radiographs. Phase 4 is for the

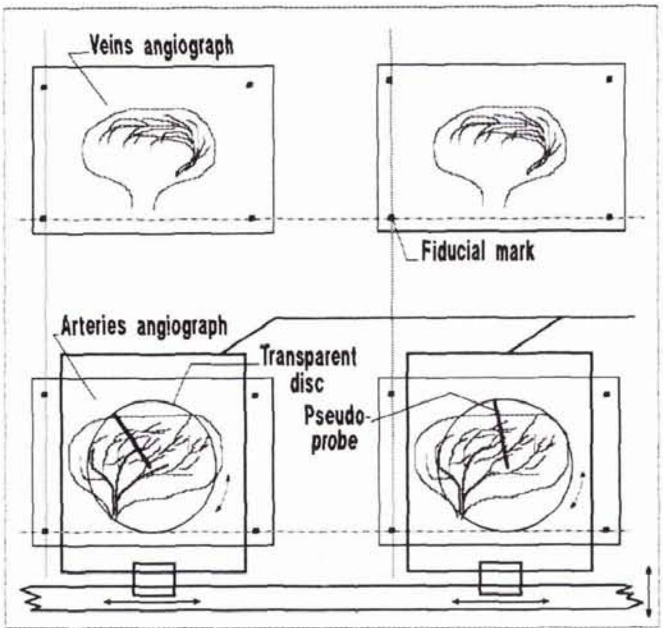

FIG. 11. Alignment of radiographs on the simulator table.

localization of the two points defining the path. The small lead balls on the angiographic cube serve as calibration points. The accuracy of these points is estimated to 0.1 mm. Because the unconventional camera has no lens and because X-rays travel almost perfectly linearly (Takamoto, 1976; Jamet, 1984), only three parameters suffice to define the inner orientation, that is, the distance between the source and the film (f) and the location of the principal point (x_O,y_O) at the surface of the radiographic film (Ghosh and Boulianne, 1984; Boulianne, 1986). The measurement of the image coordinates needed for the calibration computation is done using the digitizer included in the probe simulator (Figure 7).

The typical standard errors obtained from the self-calibration are: ± 2 mm in the 4.5-m principal distance, ± 3 mm in the position of the perspective center, and ± 0.06 degree for the attitude of the X-ray camera. With these precisions, the spatial coordinates can be estimated with an accuracy better than 0.3 mm (see section on the results). The results prove the appropriate choice of the collinearity condition in the present radiographic context. This high precision can be partially explained by the fact that, unlike conventional photographs, radiographs show the objects in about the same scale and, consequently, the propagation of the observational errors in the photo coordinates affects the object coordinates determination less severly.

PHASE 5: THE IMPLANTATION

The implantation, the last part of the procedure, is achieved according to the location and the direction established in the course of phase 4. Knowing two points of the floating line, the equation of the path is computed and the spatial intersection of this geometrical entity and the mathematical surfaces defined by the guidance frame are determined. The tool used to guide the probe is fixed to the main frame holding the patient's head and is, of course, related to the same coordinate system in which the control points are defined. Several probe guidance frames can be adapted to the technique just described. A complete description of these frames is beyond the scope of this paper. An "all azimuth" guidance frame which encompasses all the possibilities of the floating line concept together with additional qualities such as solidity, versatility, and precision has also been designed (see Figure 12).

CLINICAL RESULTS

All new procedures have to follow a long period of testing before being accepted or approved by the medical community. The present method is no exception and several tests had to be carried out before being accepted. This section will present some considerations about the precision achievable with the new system and clinical results will be discussed.

Unlike the usual photogrammetric applications, in neurosurgery there is no numerical specification of the required accuracy. Indeed, a probe implantation is considered to be successful if no internal bleeding is induced. Nevertheless, some tests were performed to evaluate the efficiency of the probe simulator. The first one consisted in evaluating the accuracy of the localization of well-defined points. For that purpose, an acrylic model having 31 lead dots was made (Figure 13). Five of these points were considered as check points and were introduced as such in the adjustment (approximate coordinates were given with a 10-cm weight). The 3-D coordinates of the check points were previously established by high precision mechanical means. One stereopair was produced with a 15 degree parallactic angle. After measuring the image coordinates at a comparator, the self-calibration technique was used to estimate the check point coordinates. Table 1 presents the results of the comparison between

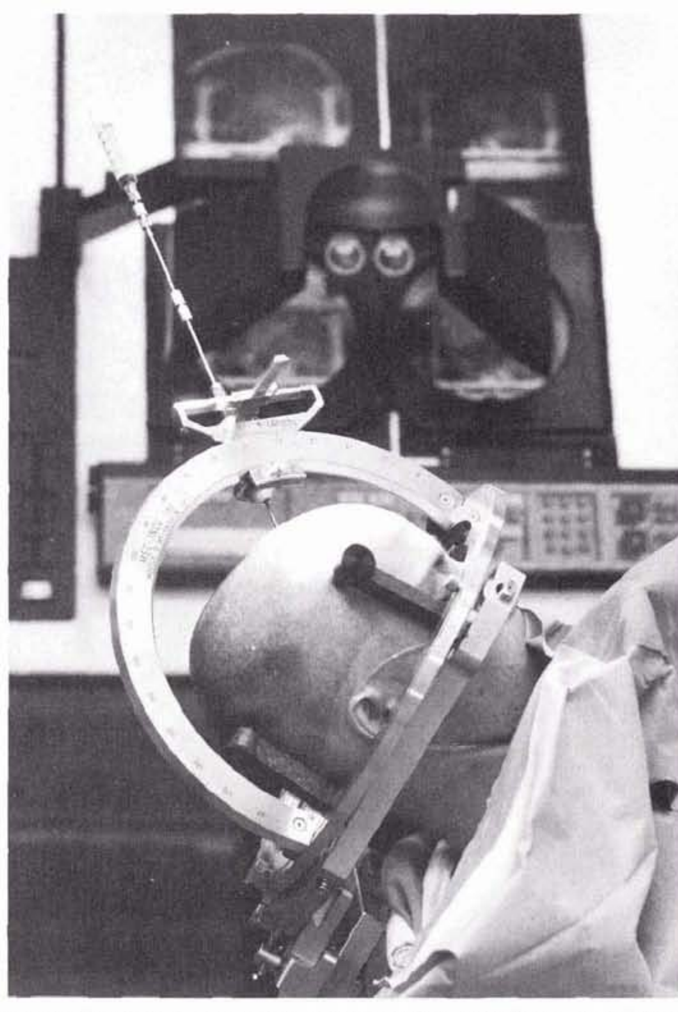

FIG. 12. Probe guidance system. (Courtesy of MEC-INOV Inc. and Enfant-Jésus Hospital)

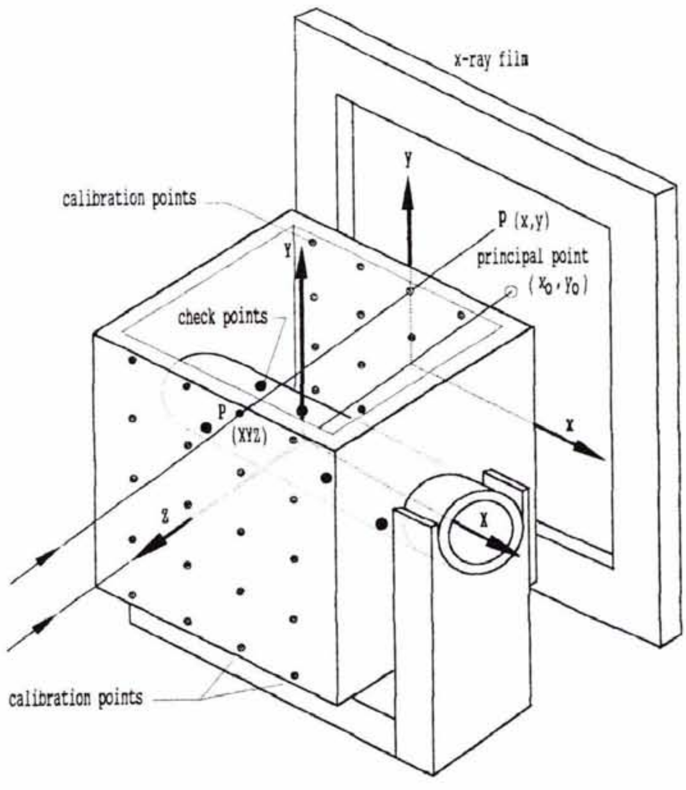

FIG. 13. Acrylic test cube.

TABLE 1. COMPARISON BETWEEN MECHANICALLY AND PHOTOGRAMMETRICALLY DERIVED COORDINATES.

Point Number	Mechanical Coordinates (mm)			Photogrammetric Coordinates (mm)			Differences (mm)		
	X	Y	Z	X	Y	Z	X	Y	Z
27	−30,0	−25,0	0,0	−30,0	−24,8	−0,1	0,0	−0,2	0,1
28	−15,0	0,0	−25,0	−15,0	0,0	24,7	0,0	0,0	−0,3
29	0,0	25,0	0,0	0,0	24,9	0,0	0,0	0,1	0,0
30	15,0	0,0	25,0	15,1	0,0	24,9	−0,1	0,0	0,1
31	30,0	−25,0	0,0	30,1	−24,8	0,0	−0,1	−0,2	0,0

the mechanically derived coordinates and the ones obtained by photogrammetry. Despite the fact that the experimental conditions were slightly different from those encountered during normal medical procedures, the results provide an idea of the achievable accuracy using the self-calibration technique in a radiographic context.

Concerning the precision of the localization of the probe, other tests were carried out. Obviously, this accuracy depends on the stereoscopic perception of the simulator operator. Different metallic models were made and implanted with a pseudo-probe. One of them was composed of metallic springs. The diameters varied from 5 mm to 20 mm, their lengths being around 5 cm each. All the probes introduced through each spring did not touch the spring itself.

Before trying the new technique on a real patient, a final test had to be done. This time the model used was a real human cerebral blood vessels network from a cadaver. To produce such a network, on anatomist introduces in the cerebral vessels a fine dust of lead amalgamed with a liquid plastic mixture which hardens rapidly. Afterwards, the brain is immersed in a substance which melts away the biological matter, leaving only the plastic structure. This is called a corroded brain. Numerous probes were again introduced in this model without touching any blood vessel.

On 5 October 1988 Dr. Claude Picard, supported by the medical staff at the Enfant-Jésus Hospital in Québec city, decided to apply the new technique on a real patient. For the first trial a patient showing a very big tumor situated in a relatively avascular part of the brain was selected. The operation took almost 7 hours but a sample of the affected grey matter was withdrawn without any internal bleeding. Since then 42 biopsies have been carried out on 25 different patients with 100 percent rate of success. Because the present technique for finding avascular paths does not require the 3-D digitization of the vessels, no other statistics, such as the minimal distance between the vessels and the probes implanted, can be established. As expertise grew, the operation time shrank from 7 to less than 4 hours for the last case. One of these cases represented a very important challenge because the tumor was very small (≈5 mm in diameter) and was located in the deepest region of the brain (near the thalamus). The neurosurgon decided to access the tumor through the top of the head. For this particular case, the conventional method for introducing a biopsy tool through the profile would have been impossible due to the high density of arteries and veins in the area if accessed by the profile.

CONCLUSION

A new method for finding safe paths for neurosurgical probes based on a special photogrammetric apparatus has been presented in this paper. This equipment has the definite advantage of offering a simple way to locate, with a high level of confidence, the safest passage for any cerebral investigation tool. Because no constraints with regard to the direction or entry of the probe exist in the new method, different parts of the brain formerly classified as inaccessible can be reached. In some cases such an investigation can be a matter of life or death.

Even though the number of operations is still relatively small, no post-operation complications have been reported, which is a source of real optimism for the neurosurgical community.

ACKNOWLEDGMENTS

The authors express sincere appreciation for the assistance received from the following: Dr. Claude Picard of the Enfant-Jésus Hospital, Dr. Guy Bouvier of the Notre-Dame Hospital, Dr. Dinh Nguyen, Mr. Pierre-Michel Arseneault and Mr. Roland Picard, of the Department of Mechanical Engineering, Mr. Louis Gosselin president of MEC-INOV inc., Mr. Paul Labissionnière formerly working for this company, Mr. Pierre Marcotte mechanical engineer, Mr. Paul Trotier and Mr. Jean Horvath of the photogrammetry laboratory. It is also important to underline the excellent technical support received from the Notre-Dame and the Enfant-Jésus Hospitals. Finally they want to thank Mr. Joël Emond, photographer at the latter institution.

REFERENCES

Arsenault, P. M., M. Boulianne, L. Cloutier, S. K. Ghosh, P. Labissionnière, P. Marcotte, and D. Nguyen, 1986. *Simulator for Use, as a Neurosurgical Aid, in Determining Potential Paths for the Implantation of Probes through the Human Body,* USA Patent No. 4.614.499, Canada Patent No. 1 246 744.

Boulianne, M., 1983. *Transformation d'une salle de radiographie conventionnelle en appareil de mesure,* M.Sc. thesis, Université Laval.

———, 1986. *Les rayons-X, l'autocalibrage et la ligne flottante dans un nouvel appareil photogrammtrique,* Ph.D. thesis, Université Laval.

Bouvier G., J. M. Saint-Hilaire, J. L. Vézina, R. Béique, and R. Picard, 1976. *La chirurgie fonctionnelle de l'épilepsie,* Union Médicale du Canada, Hôpital Notre-Dame, Montréal.

Brown, D. C., R. G. Davis, and F. C. Johnson, 1964. *The Practical and*

Rigorous Adjustment of Large Photogrammetric Nets, Report on U.S. Air Force, Contract No. AF-30(602) - 3007, DBA System Inc., Florida.

Jamet, F., 1984. La diffraction X instantanée, *High Speed Photography, Proceeding of the International Society for Optical Engineering*, Vol. 491, pp. 137–143.

Kenefick, J. F., M. S. Gyer, and B. F. Harp, Analytical self-calibration, *Photogrammetric Engineering*, Vol. 38 No. 11, pp. 1117–1126.

Ghosh, S. K., and M. Boulianne, 1984. X-ray photogrammetry and floating lines in support of neurosurgery. International Archives of Photogrammetry and Remote Sensing, Vol. 25, Commission V, pp. 325–335.

Gibaud, B., J.- M. Scarabin, B. Lorig, and C. Cruette, 1982. Accurate use of CT scanner, stereotaxis and photogrammetry for diagnosis and treatment of cerebral lesions (tumours), *International Archives of Photogrammetry*, Vol. 24, Commission V, pp. 225–233.

Marcotte, P., 1984. *Élaboration d'une méthode de mesure spatiale á partir d'un principe photogrammétrique adapté aux rayons-x*, M. Sc. thesis, Université Laval.

Sherlock, R., and W. M. Aitken, 1980. A method of precision position determination using X-ray sterography, *Phys. Med. Biol.*, Vol. 25, No. 2, pp. 349–355.

Slama, C. C, (ed.), 1980. *Manual of Photogrammetry*, Fourth Edition, American Society of Photogrammetry, Falls Church, Virginia.

Takamoto, T., 1976. *X-Ray Photogrammetric Analysis of Skeletal Spatial Motions*, Ph.D. Dissertation, University of Washington Seattle, Washington.

Talairach, J., 1974. Approche nouvelle de la neuro-chirurgie de l'épilepsie. *Neurochirurgie*, Vol. 20.

(Received 6 July 1990; revised and accepted 4 December 1990)

Forthcoming Articles

Haluk Cetin and *Donald W. Levandowski*, Interactive Classification and Mapping of Multi-Dimensional Remotely Sensed Data Using n-Dimensional Probability Density Functions (nPDF).

Yue Hong Chou, Slope-Line Detection in a Vector-Based GIS.

Raymond L. Czaplewski, Misclassification Bias in Areal Estimates.

Peter F. Fisher, First Experiments in Viewshed Uncertainty: Simulating Fuzzy Viewsheds.

G. M. Foody, A Fuzzy Sets Approach to the Representation of Vegetation Continua from Remotely Sensed Data: An Example from Lowland Heath.

Steven E. Franklin and *Bradley A. Wilson*, A Three-Stage Classifier for Remote Sensing of Mountain Environments.

Clive S. Fraser, Photogrammetric Measurement to One Part in a Million.

Daniel K. Gordon, *Paul W. Mueller*, and *Matthew Heric*, An Analysis of TIMS Imagery for the Identification of Manmade Objects.

Christian Heipke, A Global Approach for Least-Squares Image Matching and Surface Reconstruction in Object Space.

Peter E. Joria, *Sean C. Ahearn*, and *Michael Conner*, A Comparison of the SPOT and Landsat Thematic Mapper Satellite Systems for Detecting Gypsy Moth Defoliation in Michigan.

D. King, Determination and Reduction of Cover Type Brightness Variations with View Angle in Airborne Multispectral Video Imagery.

Richard G. Lathrop, Jr., Landsat Thematic Mapper Monitoring of Turbid Inland Water Quality.

Franz W. Leberl, *Kelly Maurice*, *John Thomas*, and *Wolfgang Kober*, Radargrammetric Measurements from the Initial Magellan Coverage of Planet Venus.

Donald L. Light, The New Camera Calibration System at the U. S. Geological Survey.

Hans-Gerd Maas, Digital Photogrammetry for Determination of Tracer Particle Coordinates in Turbulent Flow Research.

Ronald T. Marple and *Eugene S. Schweig, III*, Remote Sensing of Alluvial Terrain in a Humid, Tectonically Active Setting: The New Madrid Seismic Zone.

Fabio Maselli, *Claudio Conese*, *Ljiljana Petkov*, and *Raffaello Resti*, Inclusion of Prior Probabilities Derived from a Nonparametric Process into the Maximum-Likelihood Classifier.

Ram M. Narayanan, *Steven E. Green*, and *Dennis R. Alexander*, Soil Classification Using Mid-Infrared Off-Normal Active Differential Reflectance Characteristics.

Kurt Novak, Rectification of Digital Imagery.

Kevin P. Price, *David A. Pyke*, and *Lloyd Mendes*, Shrub Dieback in a Semiarid Ecosystem: The Integration of Remote Sensing and Geographic Information Systems for Detecting Vegetation Change.

Randall L. Repic, *Jae K. Lee*, *Paul W. Mausel*, *David E. Escobar*, and *James H. Everitt*, An Analysis of Selected Water Parameters in Surface Coal Mines Using Multispectral Videography.

Omar H. Shemdin and *H. Minh Tran*, Measuring Short Surface Waves with Stereophotography.

Thierry Toutin, *Yves Carbonneau*, and *Louiselle St-Laurent*, An Integrated Method to Rectify Airborne Radar Imagery Using DEM.

William S. Warner and *Øystein Andersen*, Consequences of Enlarging Small-Format Imagery with a Color Copier.

Zhuoqiao Zeng and *Xibo Wang*, A General Solution of a Closed Form Space Resection.

November 1991 Special Issue on Geographic Information Systems

D. R. Breininger, *M. J. Provancha*, and *R. B. Smith*, Mapping Florida Scrub Jay Habitat for Purposes of Land-Use Management.

L. W. Carstensen and *J. B. Campbell*, Desktop Scanning for Cartographic Digitization and Spatial Analysis.

R. N. Fernandez, *D. F. Lozano-Garcia*, *G. Deeds*, and *C. J. Johannsen*, Accuracy Assessment of Map Coordinate Retrieval.

A. U. Frank, *M. J. Egenhofer*, and *W. Kuhn*, GIS Technology in the Nineties.

T. R. Loveland, *J. W. Merchant*, *D. Ohlen*, and *Jesslyn F. Brown*, Development of a Land-Cover Characteristics Database for the Conterminous U. S.

D. M. Mark and *M. Gould*, Interacting with Geographic Information: A Commentary.

Parker H. Dennison, Commentary: The Role of the Private Sector in GIS.

J. M. C. Pereira and *R. M. Itami*, GIS-Based Habitat Modeling fot the Mt. Graham Red Squirrel Using Logistic Multiple Regression.

S. Zhuang, *B. A. Engel*, *M. F. Baumgardner*, and *P. H. Swain*, Improving Classification for Crop Residues Using GIS-Enhanced Landsat TM Data.